Biochimica et Biophysica Acta 816 (1985) 332–348
Elsevier

BBA 72642

Formation and properties of aqueous leaks induced in human erythrocytes by electrical breakdown

K. Schwister * and B. Deuticke

Abt. Physiologie, Medizinische Fakultät der Rheinisch-Westfälischen Technischen Hochschule, Pauwelsstrasse, D-5100 Aachen (F.R.G.)

(Received December 27th, 1984)

Key words: Erythrocyte membrane; Ion selectivity; Ion pore; Electrical breakdown; Membrane permeability

Leaks were induced in human erythrocytes by brief (τ = 1–40 μs) discharges of high electric fields (3–20 kV/cm). Leak permeabilities were characterized by measuring (a) net and tracer fluxes of K^+ and nonelectrolytes under protection of the cells against colloid-osmotic lysis, or (b) rates of colloid osmotic lysis in various salt solutions. The induced permeabilities are essentially stable for hours at 0–2°C. Leak permeability P increases exponentially with the breakdown voltage E_D according to a function of the general type $P = b^{E_D}$. The basis b varies with the pulse length. A log-linear presentation reveals a biphasic linear relationship with a break at which the slope (= log b) decreases markedly. Elevated ionic strengths of the suspension medium during the electric discharge enhance leak formation. Leak permeability exhibits an apparent activation energy of 29 ± 5 kJ/mol, indicative of diffusion through aqueous pathways. Somewhat differing equivalent pore radii emerge from measurements with different probes: 0.6–0.8 nm from tracer fluxes of polyols (M_r = 3600, E_D = 4–7 kV/cm) and 0.8–1.9 nm from osmotic protection studies with polyethylene glycols (M_r = 200–3300, E_D = 6–10 kV/cm). These numbers and the non-monoexponential increase of leak permeability with the field strength suggest a dual mechanism for the increase of leak permeability: an increase of the number of pores at low breakdown voltage and an additional increase of pore size at higher voltage. Estimated numbers of pores range from 1 to 10 per cell, which suggests dynamic fluctuating structural defects to be involved. The leaks discriminate small monovalent inorganic ions in the sequence of free solution mobility. Organic anions are discriminated according to size and charge. Common properties of these electrically induced defects and of chemically induced leaks (diamide, periodate, t-butylhydroperoxide) in the erythrocyte membrane suggest close similarities in the molecular organization.

Introduction

The barrier function of artificial lipid membranes and of biological membranes can be disrupted reversibly by brief electric discharges which raise the transmembrane potential to values greater than 1 V [1]. In pure lipid systems, the breakdown leads to very short-lived states of highly elevated conductance which renormalize with half-times in the μs range [2,3]. A number of models have been put forward to explain the molecular events underlying the formation of the short-lived defects [1,2–6]. Their functional properties are not well-characterized.

Electrical breakdown of biological membranes frequently goes along with the occurrence of much more stable states of increased permeability [7–12]. The lifetime of the induced leaks is long, in particular, when the cells are kept at low temperature

* To whom correspondence should be addressed.

Abbreviation: r_{SE}, Stokes-Einstein radius.

after breakdown [7,8,13,14]. The induced leaks are permeable to small ions, but not to large intracellular solutes [1,7,8]. Therefore, electric breakdown leads to colloid-osmotic lysis [15] of the perforated cells. This type of lysis can be prevented by addition, to the extracellular phase, of impermeant solutes which compensate for the osmotic pressure of the intracellular impermeant polyelectrolytes [8]. Due to these two features, stability of the induced leaks at low temperature, and stability of the leaky cells in the presence of macromolecular additivities, the properties of electrically induced leaks are accessible to experimental characterization.

A major object of studies concerning electric breakdown of biomembranes has been the erythrocyte [1,7–9,13,14], in which the release of ions and of hemoglobin can easily be monitored. From earlier studies it has become evident that leak formation increases with increasing external field strength (> 2 kV/cm) and pulse length [7–9]. The details of this relationship, however, are still unknown. Moreover, it was claimed that the increase of leak permeability might be due to an increase of pore size [9]. Whether or not the number of pores (per cell) also depends on field strength or pulse length is yet unclear. Finally, the apparent size of the induced leaks, and their ability to discriminate ions and non-electrolytes have not been investigated in detail. In the course of a series of studies dealing with the properties of leaks induced in the erythrocyte membrane by chemical and physical alterations [16–18] we have therefore investigated these problems and also analysed in detail the field-strength and pulse-length dependence of the induced permeability by quantitative kinetic measurements. Preliminary results have been published elsewhere [19].

Materials and Methods

Fresh human blood was obtained at least weekly from the local blood bank and anticoagulated by heparin. After removal of plasma and buffy coat, the erythrocytes were washed three times in 10 vol. isotonic NaCl. Packed cells were then suspended at a hematocrit of 30% in a medium (medium A) containing (in mM): KCl (115), NaCl (25), Dextran 4 (Serva GmbH, Heidelberg) (30), imidazole (1), pH 7.4. 10 ml of this suspension were cooled to 0°C, filled into a discharge chamber originally developed by Riemann et al. [7] and exposed to a brief, exponentially decaying pulse ($\tau = 1$–40 μs) of high voltage (3–20 kV/cm) by means of a discharge equipment with a spark gap as a switch. The time constant τ of the pulse was taken as $R \cdot C$, where R is the ohmic resistance of the suspension and C the capacitance of the storage capacitors. After the discharge, the cells were kept strictly at 0–2°C until further use.

Measurement of K^+ efflux

In order to assess the K^+ permeability of leaky cells, K^+ net efflux rates were determined by following the appearance of K^+ in the suspension medium by means of an ion-sensitive electrode. Following the discharge, the cells were spun down ($12\,000 \times g$) in a refrigerated centrifuge (Sigma 2 MK) and mixed rapidly, by a special injection device, into 50 vol. of the following ice-cold medium (mM): choline chloride (140), Dextran 4 (30), imidazole (1), pH 7.4. The K^+ activity in this medium was measured continuously by a K^+-sensitive combined glass electrode (Ingold PK 401-NS-K 7). In this electrode, the reference electrolyte compartment containing 3 M KCl is coupled to the solution to be analysed by a bridge compartment containing Tris-sulfate. K^+ contamination of the incubation medium is thus avoided. The electrode was connected to a recorder and to a computer (Apple II plus) for storage of the voltage output of the electrode at intervals selected depending on the expected time-course of K^+ efflux.

Changes of voltage (K^+ concentrations) were followed to about 95% of completion. The maximum voltage, after equilibration of K^+ between leaky cells and medium, was then obtained by lysing the cells with a small volume (100 μl) of Triton X-100. The stored voltage data were converted into K^+ concentrations using standard solutions as a reference and corrected for the amounts of extracellular potassium carried into the system upon addition of packed cells. Rate coefficients k of K^+ efflux were obtained by evaluation of the data in terms of two-compartment kinetics by the equation:

$$\ln\left(1 - \frac{K_e^+}{K_\infty^+}\right) = -k \cdot t$$

Measurements of rates of hemolysis

Discontinuous procedure. The permeability of leaky erythrocytes to ions or salts, respectively, can also be determined by following the time-course of colloid-osmotic hemolysis occurring upon suspending the cells in electrolyte solutions not containing impermeable solutes to counterbalance the colloid-osmotic pressure of hemoglobin (see Ref. 17). In the experiments, 100 μl packed cells (0°C), obtained by centrifugation of the cell suspension after breakdown, were squirted rapidly into 6 ml of various isotonic (300 mosmol/l) salt solutions at 0–2°C. After various time intervals, the extent of hemolysis was determined by measuring the hemoglobin content in the supernatant as cyanmethemoglobin and relating this value to the total hemoglobin content of the cell suspension.

Continuous procedure. Rates of rapid hemolysis can also be measured by following the changes of light scattering or absorbance of a very dilute cell suspension during hemolysis. 50 μl of a cell suspension in medium A, subjected to electric pulses as described above, were mixed rapidly into a photometric cuvette (path length 1 cm) containing 2.5 ml isotonic salt solution maintained at 0°C. The suspensions were stirred by a magnetic stirrer and changes of absorbance at 700 nm registered on a recorder. The change of the signal is proportional to the extent of hemolysis.

Both techniques provide half-times of hemolysis (i.e., the time required for the release of 50% of the hemoglobin). The reciprocal of this value served as a 'rate coefficient'.

Measurements of tracer fluxes

In order to obtain permeabilities on an absolute scale, tracer fluxes were measured in cells after dielectric breakdown. To this end, the cells were suspended in medium A containing in addition the test permeant at a concentration of 4 mM (= medium B) and loaded with labelled test permeant at 0°C for 2 h. The loaded cells were spun down and washed once in medium B. Tracer efflux was started by resuspending the cells in medium B. Changes of supernatant radioactivities were determined and fluxes or permeabilities computed as described [16].

Results

Human erythrocytes subjected to short pulses of high voltage and subsequently suspended in an isotonic solution of an electrolyte can be protected against lysis by a solute unable to enter the cells via the electrically induced leaks. In preliminary experiments, it was established that Dextran 4 (M_r 4000–6000) and poly(ethylene glycol) 4000 did not only prevent lysis but also colloid-osmotic swelling of erythrocytes during a period necessary to measure K^+ leak fluxes. These additives were therefore used in all experiments in which lysis was to be avoided. Protectants with higher molecular weights were used only in particular instances.

Characteristics of leak formation

Net fluxes of K^+

The time-course of the loss of K^+, into choline chloride medium, from cells subjected to a 40 μs, 5 kV/cm pulse is shown in Fig. 1 which presents the

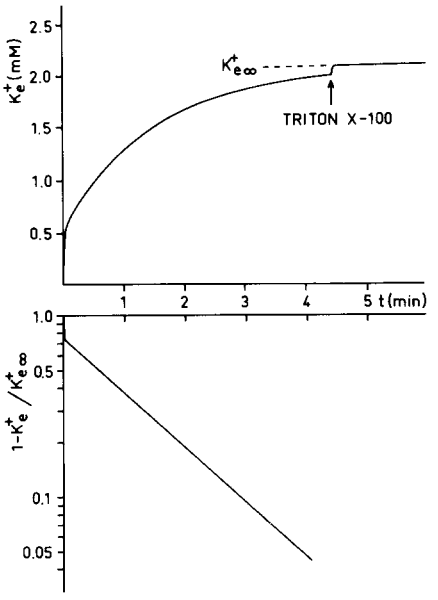

Fig. 1. Release of K^+, from human erythrocytes subjected to an electric pulse ($\tau = 40$ μs) of 5 kV/cm, into a choline chloride medium containing 30 mM Dextran 4 to protect cells against colloid-osmotic lysis. $T = 0$°C. Increase of K^+ in the suspension medium represented in a linear and a semilogarithmic diagram. K^+ concentrations measured continuously by an ion-selective electrode as described in Materials and Methods.

increase of extracellular K^+ and the semilogarithmic kinetics of K^+ efflux derived therefrom. Similar curves were obtained for other breakdown voltages. At all voltages applied in our study all cells become leaky, as indicated by identical K^+ values when either the leak flux was allowed to proceed until equilibrium or complete K^+ equilibration was obtained by lysing the cells with Triton-X 100 (data not shown). The slopes of the efflux curves were independent of the cell content of the suspensions during breakdown up to a hematocrit of 30%, indicating that the effects of the electric discharge are not influenced by the cell density up to this value.

Since the response time of the electrode at 0°C is 2 s for 90% and 5 s for 95% equilibration at a K^+ concentration jump of 0.3 mM, the curve represents the true time-course of changes of extracellular K^+. The initial steep phase in the original graph and in the semilogarithmic evaluation result from the introduction of extracellular K^+ into the suspension medium at the start of the experiments. The semilogarithmic plots were linear up to at least 90% equilibration, indicating that the system behaves as a homogeneous two-compartment system. Rate coefficients k obtained by this procedure were reproducible for cells from different donors and from day to day at a level of $\pm 10\%$. Moreover, the rate coefficients remained essentially the same when the leaky cells were stored at 0–2°C for a time period up to 4 h after breakdown. Prolonged storage on ice went along with some resealing of the leaks in spite of low temperature.

The rate of K^+ efflux increases overproportionally with increasing breakdown voltage (Fig. 2A). The measured time-constants range from 0.1 to 10 min^{-1}, equivalent to half-times between 10 min and 6 s. The shape and the position of the curves vary with the length of the electric pulse. With decreasing time constants τ, the curves were shifted to higher field strengths and also exhibit a lesser slope.

In an attempt to linearize these curves for a numerical evaluation, a log-linear presentation provided the best results (Fig. 2B). A biphasic linear relationship was obtained with a break at which the slope decreased markedly. Below and above the break the relationship follows a function

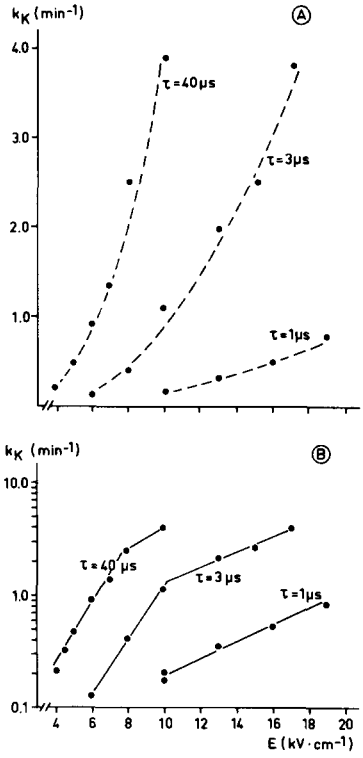

Fig. 2. Voltage dependence of the rate of K^+ efflux from erythrocytes subjected to electric pulses. Rate coefficients, plotted in a linear (A) and log-linear (B) fashion against applied voltage, for time constants τ varying from 1 to 40 μs. Data points are mean values from 2–4 experiments. Note the biphasic linear relationship with a break in the semilogarithmic plot.

of the general type:

$$\log y = x \cdot \log b \tag{1}$$

(the logarithmic form of $y = b^x$). For the special situation of this study, in which we analysed the changes of leak flux rate k with increasing voltage E_D in the range above a critical breakdown voltage E_{crit}, the appropriate equation is:

$$\log \frac{k}{k_{crit}} = (E_D - E_{crit}) \cdot \log b \tag{2}$$

The value of b can easily be obtained from the ratio of k values per unit increase of E_D, i.e. per 1 kV/cm. In the region below the break, b equals 1.8 (at $\tau = 40$ and 3 μs). Above the break, it decreases to 1.2–1.3. The ratio of the b values is

thus about 1.5. At $\tau = 1$ μs, no break was observed. This may result from the real lack of a break at this short pulse length but could also be due to the impossibility to apply voltage pulses greater than 20 kV/cm in our experimental setup.

The K^+ efflux rate coefficients for cells after electric breakdown can be compared to those of K^+ loss from native cells. Under our experimental conditions we obtained a value of about 0.001 min^{-1} ($= 0.06$ h^{-1}) for native cells, somewhat higher than a rate coefficient, for the electro-diffusive K^+ leak, of 0.006 h^{-1} estimated by Glynn [20]. Even at the lowest breakdown voltages applicable with out equipment, the K^+ loss is thus already enhanced by at least two orders of magnitude (8.4 h^{-1} at 3 kV/cm vs. 0.06 h^{-1}).

Rates of colloid osmotic hemolysis

The relationship between induced leaks and inducing field strength can be assessed by measuring the rates of hemolysis in isotonic NaCl solution at 0°C. Lysis of cells after electrical breakdown occurs more slowly than K^+ efflux. At 5 kV/cm and $\tau = 40$ μs, e.g., the half-time of K^+ loss is about 1.5 min, that of hemolysis (in NaCl), however, 15 min. The most likely reason for this difference are the very different driving forces, i.e., the distances of the K^+ concentration and of the colloid-osmotic pressure from their respective equilibria. Generally, the lysis technique allowed measurements over a larger range of voltages. As in the case of the induced K^+ leak, half-times of lysis remained constant for the leaky cells for about 4 h at 0°C after breakdown.

Rates of hemolysis, defined as the reciprocal of the half-time for lysis, also increase exponentially with breakdown voltage (Fig. 3). The slopes are about twice as steep as those for K^+ fluxes in Fig. 2. The reason for this difference is yet unclear. There was also a gradual decrease of the slope with decreasing pulse length and a concomittant shift of the curves to higher voltages. Values of b below the break decrease with decreasing pulse length from 3.5 ($\tau = 40$ μs) to 2.1 ($\tau = 3$ μs). Above the break, the numbers are 1.6 and 1.3, respectively. The ratio of the b values above and below the break ranges from 2.3 to 1.6. From these more extended studies it also became evident that the position of the breaks seems to be related

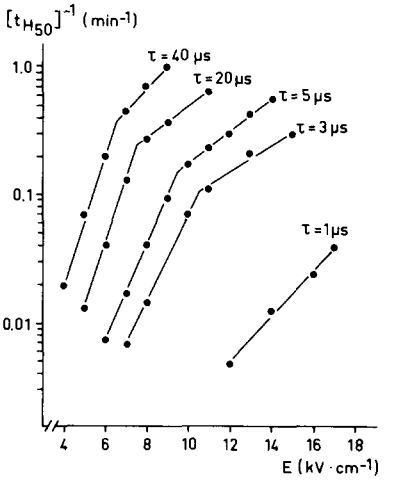

Fig. 3. Voltage dependence of electrically induced leak permeabilities derived from rates of colloid-osmotic lysis at 0°C in isotonic NaCl solutions. Leak permeabilities defined as the reciprocal of the half-time of hemolysis. For experimental procedure see Material and Methods. The relationship exhibits a break at a critical voltage, varying with the pulse length.

neither to a critical value of E_D nor to a critical value of the leak permeability. Again, at $\tau = 1$ μs there was no break detectable.

Tracer fluxes

Rates of hemolysis are a somewhat indirect measure of leak permeability and not easy to safeguard against artifacts. We therefore attempted to ascertain the break in the permeability/breakdown voltage relationship by complementary studies using a different technique. According to Fig. 4, the leak permeability of a nonelectrolyte, erythritol, derived from tracer fluxes at chemical equilibrium in osmotically protected cells, increases with E_D in the same way as do K^+ fluxes. Moreover, there is also a break in the relationship at about the same voltage (for $\tau = 40$ μs), at which it was observed for the other test permeants. The values of b correspond to those for K^+ fluxes, i.e., 1.9 below and 1.4 above the break. Similar results were obtained for other nonelectrolytes, e.g. sucrose and mannitol.

Influence of ionic strength

In a former study [9] it was claimed that an increase of the ionic strength of the medium in

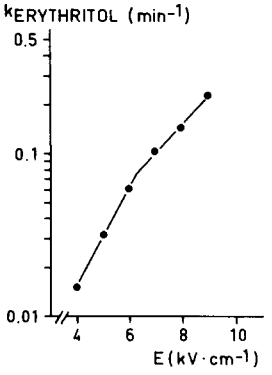

Fig. 4. Voltage dependence of the electrically induced leak permeability for erythritol at 0°C as measured by tracer fluxes at chemical equilibrium. Cells were protected against colloid-osmotic lysis by 30 mM Dextran 4. The permeability/breakdown voltage relationship exhibits a break at about 6 kV/cm. Mediated transport of erythritol blocked by cytochalasin B, 10 μM.

which cells are suspended during breakdown markedly diminishes the extent of the electrically induced leak permeability. In that study, however, changes of the ionic strength went along with changes of the ohmic resistance of the suspension medium and consecutive changes of the discharge time constant $\tau = R \cdot C$ of the system.

Specially designed media allow to distinguish between effects of ionic strength and of ohmic resistance. We used isotonic solutions of various multivalent ions and could demonstrate (Table I), that a selective increase of the ionic strength of the breakdown medium, without a concomittant change of its ohmic resistance, increases the induced leak permeability. This effect was independent of the ion species used. In view of these results, it is likely that the increase of leak permeability reported by others [9] upon a decrease of the ionic strength of the breakdown medium was due to a concomittant decrease of the discharge time, resulting from a decrease of the ohmic resistance of the suspension medium. We could demonstrate that the induced leak permeability is diminished when the ohmic resistance of the breakdown medium is lowered at constant ionic strength (compare line 1 and 2 of Table I).

Increasing ionic strength increases the induced leak permeability at all voltages tested. The position of the break in the log-linear relationship remains essentially unaltered (Fig. 5). The ionic strength of the pulse medium thus does not seem to affect the processes responsible for this break.

TABLE I

INFLUENCE OF THE IONIC STRENGTH AND THE OHMIC RESISTANCE OF THE SUSPENSION MEDIUM DURING ELECTRICAL BREAKDOWN ON FIELD-INDUCED LEAK PERMEABILITY

Cells (hematocrit = 30%) were subjected to electric pulses (6 kV/cm) in the media described in column 1, containing in addition Dextran 4 (30 mM) and imidazole (1 mM). Subsequently, they were transferred into medium A (see Materials and Methods) at 0°C for 1 h to establish the same intracellular ionic condition in all samples. Rates of colloid-osmotic lysis were then determined as usual. (R = ohmic resistance of the suspension in the discharge chamber.)

Breakdown medium	Concn. (mM)	Ionic strength	R (Ω)	τ (μs)	k_{lysis} (normalized to KCl/NaCl)
KCl NaCl	115 25	0.14	10	40	1.00
$MgSO_4$ Sucrose	35 210	0.14	67	270	11.20
Na_2SO_4	93	0.28	10	40	2.50
$K_3Fe(CN)_6$ Sucrose	56 56	0.36	10	40	3.00
$MgSO_4$	140	0.56	10	40	4.45
$K_4Fe(CN)_6$	56	0.56	10	40	4.25

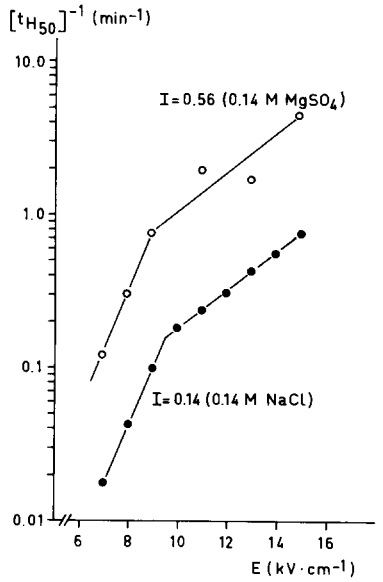

Fig. 5. Influence of the ionic strength I of the suspension media during electrical breakdown. Leak permeabilities defined as the reciprocal of the half-time of colloid-osmotic lysis in NaCl medium (●) ≙ NaCl ($I = 0.14$), (○) ≙ $MgSO_4$ ($I = 0.56$), $\tau = 5$ μs, $T = 0$°C. The break occurs at about 9 kV/cm in both cases.

Properties of the induced leak

In view of its marked electrolyte permeability, indicated by the rapid hemolysis in saline media, the induced leak is likely to be an aqueous pathway. This assumption implies a number of properties which can be tested experimentally. They comprise a low activation energy, discrimination of solutes according to size, and ion selectivity.

Temperature dependence of permeability

The influence of temperature could only be determined at low temperatures since these leaks reseal with a high-temperature dependence [19] and will not be constant for the time period required for flux measurement at temperatures above 15°C. From rate coefficients of K^+ efflux obtained, at 0, 5, 10 and 15°C, after a breakdown at 6 kV/cm and $\tau = 40$ μs, an Arrhenius activation energy of 29 ± 5 kJ/mol (7 ± 1 kcal/mol, $n = 4$) was calculated.

Apparent pore size

Information on the size of the leaks can be obtained from their permeabilities to small nonelectrolytes. Permeabilities of polyhydroxy compounds of increasing size, derived from tracer fluxes at constant cell volume are compiled in Table II. According to these data, the permeability of each of the probes increases with increasing breakdown voltage, while the ratio among the four values is not different at 6 and 8 kV/cm. As evident, the induced leak is permeable to sucrose, indicating an apparent pore radius of at least the radius of this solute.

A somewhat different approach was taken in another set of experiments. Colloid-osmotic lysis of cells leaky to anions and cations can be retarded or even prevented by addition of solutes permeating only slowly, or not at all. The osmotic pressure set up by these compounds will balance the colloid-osmotic pressure of hemoglobin. Cells 'protected' by a compound permeating the leak only slowly will finally undergo lysis, while a solute just unable to pass the leak will protect for virtually unlimited time. This strategy cannot be used in its pure form with erythrocytes after electrical breakdown since even at 0°C these cells reseal with a half-time of about 8 h. Using oligosaccharides, polyethylene glycols, and dextrans of increasing molecular weight (200–3300) it could nevertheless be demonstrated (Fig. 6) that com-

TABLE II

NONELECTROLYTE PERMEABILITIES OF ERYTHROCYTES SUBJECTED TO ELECTRIC FIELD PULSES OF A PULSE LENGTH $\tau = 40$ μs

After exposure to the field pulse as described in Materials and Methods, the cells were loaded at 0°C with labelled nonelectrolyte in media containing a high-molecular-weight protectant (Dextran 4 or 10). Subsequently the efflux of the label was measured as described in Materials and Methods and Ref. 16. Permeabilities calculated from the first-order rate constants by standard procedures [16].

	Permeability (10^{-7} cm·s^{-1}) at 0°C after breakdown at	
	$E = 6$ kV·cm^{-1}	$E = 8$ kV·cm^{-1}
m-Erythritol	0.49 ± 0.02	1.09 ± 0.15
D-Arabinose	0.29 ± 0.03	0.67 ± 0.14
Mannitol	0.19 ± 0.04	0.40 ± 0.06
Sucrose	0.04 ± 0.01	0.08 ± 0.02

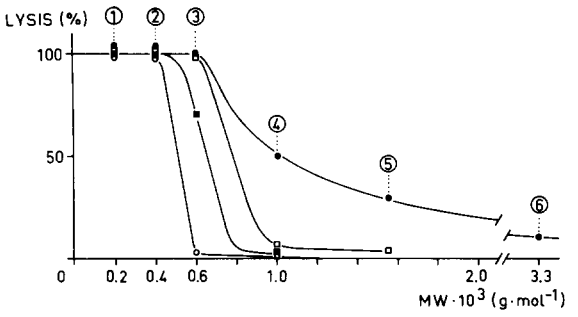

Fig. 6. Protective action of nonelectrolytes of increasing molecular size against colloid-osmotic lysis. Cells were subjected to electric pulses ($\tau = 40$ μs) at varying field strengths (○) 4 kV/cm, (■) 6 kV/cm, (□) 8 kV/cm, (●) 10 kV/cm in the usual medium containing 30 mM Dextran 4 as colloid-osmotic protectant. Subsequently, they were incubated at 0°C for 20 h in media containing the various protectants at 30 mM. The lysis observed after this incubation is plotted against the radii [21] of the test molecules (1) PEG 200, $r_{SE} = 0.56$ nm; (2) PEG 400, $r_{SE} = 0.68$ nm; (3) PEG 600, $r_{SE} = 0.80$ nm; (4) PEG 1000, $r_{SE} = 1.00$ nm; (5) PEG 1550, $r_{SE} = 1.20$ nm; (6) PEG 3300, $r_{SE} = 1.9$ nm. PEG, poly(ethylene glycol).

pounds of increasing molecular weight are required to protect cells after pulses at increasing voltages.

Ion selectivity

Inorganic ions. To evaluate the discrimination of ions by the induced pores, rates of colloid-osmotic lysis after breakdown were studied in media of varying electrolyte composition. Although salts are the migrating species in this situation, one can obtain information on the relative permeabilities of ions by keeping the counterion species constant [17].

From the data in Fig. 7A it becomes evident that the induced leaks discriminate only very little between alkali chlorides. Penetration rates increase slightly in the sequence of increasing crystalline radii of the cation. In contrast, more pronounced discrimination is observed between the halide anions (Fig. 7B). NaI, which has the largest crystal radius, penetrates about 6-times faster than NaF, having the smallest radius. These selectivities are independent of the amplitude or the length of the voltage pulse. Moreover, the breaks in the voltage response curves are observed at the same voltage, independent of the test permeant (Fig. 8).

To validate our findings it was also ascertained that the different half-times of lysis for the sodium halides were not caused by ion-dependent variations of the critical hemolytic volume of the erythrocytes. Such variations might affect the time-course of lysis independent of the permeability of the salt under investigation. We could demonstrate (data not shown) that osmotic fragility

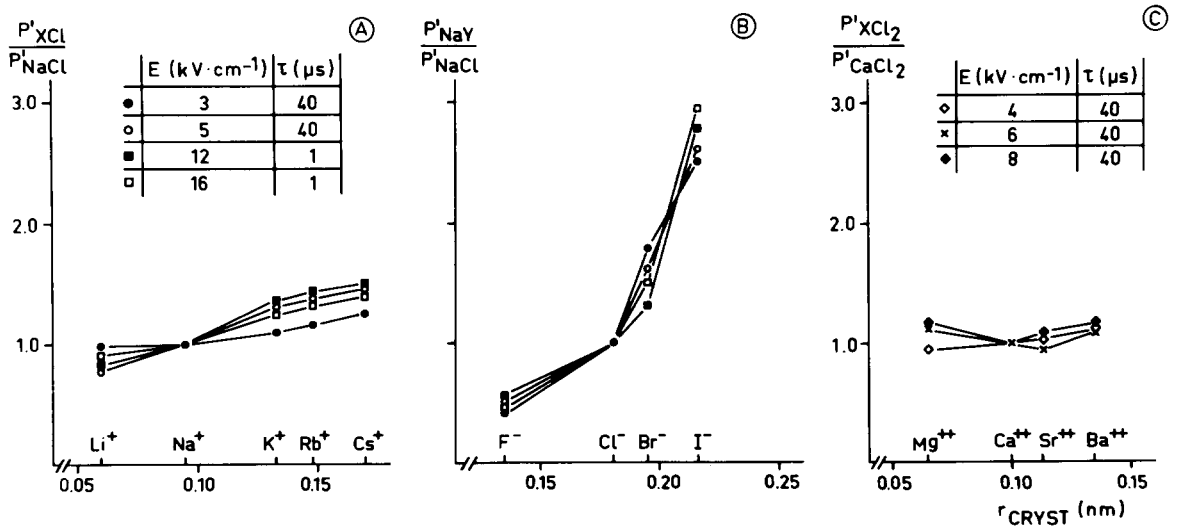

Fig. 7. Ion selectivities of leaks induced by electric pulses as derived from rates of colloid-osmotic lysis in various salt media sharing one ion and differing in the counterion. Data (P' = reciprocal half-time of lysis) normalized to the rates of lysis in either NaCl or $CaCl_2$.

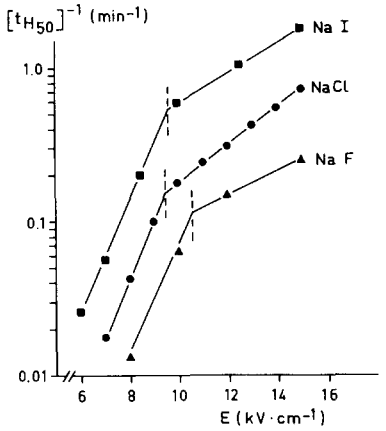

Fig. 8. Independence of the break (at $\tau = 5$ μs) in the leak permeability/field strength relationship on the salt used as test permeant. Leak permeabilities defined as the reciprocal of the half-time of colloid-osmotic lysis (at 0°C).

curves for slow, gradual hyptonic lysis were identical in solutions of a number of monovalent salts (e.g., NaI, NaCl, sodium acetate) which cause lysis of cells after electric breakdown at very different rates. Since in pores induced by chemical modification of the erythrocyte membrane the pore properties are influenced by the anion milieu [17,18], we also measured nonelectrolyte tracer permeability in leaky cells suspended in media of varying ionic composition. For electrically induced leaks, no ion dependence of leak permeability could be demonstrated (data not shown).

Alkali earth chlorides are not discriminated at all by the electrically induced leak (Fig. 7C). Their relative rates of permeation, however, are about 10-times lower than those of the alkali chlorides.

Organic anions. In view of the discrimination observed among monovalent inorganic anions, the selectivity studies were extended to organic anions (Table III). The induced leak discriminates between mono- and dicarboxylates of equal chain length and in each class between members with different chain lengths. The differences within each class are likely to be due to differences in size. The pK' values of the monocarboxylates are essentially equal and those of the dicarboxylates are not very different from each other (with the exception of

TABLE III

DISCRIMINATION OF ORGANIC ANIONS BY THE LEAKS IN ERYTHROCYTES SUBJECTED TO ELECTRIC BREAKDOWN

Cells were exposed to the field pulse ($\tau = 40$ μs) under standard conditions. Subsequently, cells were resuspended in isotonic solutions of the sodium salts of the various anions. Rates of colloid-osmotic lysis were determined as described in Materials and Methods. Bulk diffusion coefficients given for reasons of comparison are from Refs. 37 and 38.

	$(t_{H_{50}})^{-1}$ (10^{-2} min^{-1})				Diffusion coefficients	
	$E = 6$ kV·cm^{-1}	$E = 8$ kV·cm^{-1}	Normalized	$E = 10$ kV·cm^{-1}	10^{-5} cm^2·s^{-1}	Normalized
Monocarboxylates						
Chloride	20.00	67.0	–	150.0	–	–
Acetate (C_2)	1.40	4.5	1.00	10.0	1.090	1.000
Propionate (C_3)	0.79	3.2	0.71	–	0.954	0.875
Butyrate (C_4)	0.65	2.3	0.51	–	0.935	0.858
Valerate (C_5)	0.46	1.5	0.33	–	0.890	0.817
Capronate (C_6)	0.41	1.1	0.24	–	0.810	0.743
Dicarboxylates						
Sulfate	0.38	1.85	–	5.50	–	–
Oxalate (C_2)	0.53	1.43	1.00	3.33	0.980	1.000
Malonate (C_3)	0.42	1.05	0.73	2.63	0.890	0.908
Succinate (C_4)	–	0.84	0.59	2.04	0.812	0.829
Glutarate (C_5)	–	0.67	0.47	1.47	0.758	0.773
Adipinate (C_6)	–	0.45	0.32	1.22	0.705	0.719

oxalate and malonate) [22]. Leak permeabilities of mono- and divalent anions having the same number of C atoms, and therefore a comparable size, differ by a factor of about 2–3. The lower permeabilities of the dicarboxylates are probably due to the influence of their additional negative charge. Surprisingly, monocarboxylate permeation through the induced leaks is generally much slower than chloride permeation. Sodium acetate is taken up 10–20-times slower than NaCl in cells subjected to breakdown voltages between 6 and 10 kV/cm. In case of divalent anions, there is no such conspicuous difference. The sulfate permeability of the induced leak is of the same order of magnitude as its permeability to oxalate.

Particular chemical properties may also influence the discrimination between organic anions (Table IV): in monocarboxylates, an α-oxo group enhances, an α-hydroxyl group reduces the rate of permeation while a substituting Cl in the α-position is ineffective. With the dicarboxylates, substitutions have little influence with the exception of oxo groups, that have an accelerative effect (see in particular succinate) and of the two isomeric unsaturated analogous of succinate, fumarate and maleinate.

Discussion

Formation of reversible leaks in biological membranes by electrical breakdown is of considerable theoretical and potentially practical interest. From a theoretical point of view, it would be revealing to understand, why the exposure of cells to a very short field pulse will induce stable, long-lived, but still almost fully reversible membrane defects, and which membrane constituents form these defects. For practical purposes, the formation of reversible openings of predictable and controllable size in the membrane of a whole cell without chemical modification might improve techniques of the use of red blood cells as vehicles

TABLE IV

INFLUENCE OF STRUCTURAL PROPERTIES OF ORGANIC IONS ON THEIR RATES OF PERMEATION THROUGH THE LEAKS INDUCED BY ELECTRIC FIELD PULSES

Experimental details as described in Table III.

	R_1	R_2	$[t_{H_{50}}]^{-1} \cdot 10^{-2} \cdot \text{min}^{-1}$	Normalized
Butyrate	−H		5.2	1.00
α-Hydroxybutyrate	−OH		2.8	0.55
β-Hydroxybutyrate	−OH		2.9	0.57
γ-Hydroxybutyrate	−OH		3.5	0.67
α-Chlorobutyrate	−Cl		5.6	1.09
α-Oxobutyrate	=O		8.6	1.67
	R_1	R_2		
Succinate	−H	−H	0.84	1.00
	$-NH_2$	−H	0.71	0.84
$H-C(COO^-)-R_1$	−Cl	−H	0.71	0.84
$H-C(COO^-)-R_2$	−SH	−H	0.83	0.99
	−OH	−H	0.83	0.99
	−OH	−OH	0.80	0.95
Oxosuccinate			4.81	5.73
Fumarate (*trans*)			1.26	1.50
Maleinate (*cis*)			1.21	1.44
Ethanedisulfonate			1.00	1.19
Glutarate			0.67	1.00
α-Oxoglutarate			1.05	1.58

[10] for bio-active materials (drugs, etc.).

Earlier interest concerning the formation of these leaks has already been focussed on the erythrocyte [1,7–9,13,14], since electrically induced leaks in some other cells are much less stable and reseal spontaneously even at low temperatures [23,24]. These earlier studies in particular dealt with the critical breakdown voltage, i.e., the lowest voltage inducing an increase of permeability, and its variation over the cell population. Only little data were obtained for the voltage dependence of permeability changes at supercritical voltages. In most of the studies, the degree of hemolysis or the uptake of a probe molecule, determined at one fixed time interval following breakdown, served as a measured of the induced leak. Since cells were usually kept at temperatures at which resealing of the leaks is not negligible, quantitative details of such measurements cannot be evaluated. In our present study, permeabilities of cells after breakdown were assessed under defined conditions. From the results a number of conclusions can be drawn concerning the induced leaks.

Voltage dependence

(a) Leaks produced by a voltage pulse supercritical for all cells of the population are distributed homogeneously over all cells of the population. This follows from the simple two-compartment behavior of the cell suspensions during leak flux measurements.

(b) The induced leak permeability increases exponentially with breakdown voltage. This type of relationship may suggest that leak formation involves an avalanche-type or cooperative process. The parameter b (the antilogarithm of the slope) in Eqn. 2, is thus something like an amplification factor.

Its numerical values are of the order of 1.5–3 below the break and decrease to values of 1.2–1.3 above the break. The physical meaning of these numbers remains to be elucidated, since at present there is no conclusive hypothesis which can account for the formation of stable structural defects in biomembranes after breakdown, in contrast to the advanced, well-founded concepts concerning the formation of short-lived structural defects in lipid membranes after electrical breakdown [1,5,6]. It is interesting to note that in pure lipid membranes,

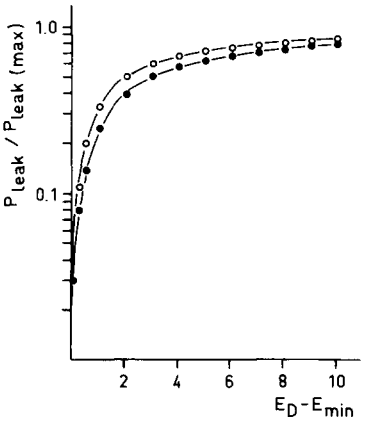

Fig. 9. Increase of the leak permeability as a function of the leak-inducing field strength as predicted by a geometric model (see Appendix). The model relates the increase of leak permeability to an increase of the fraction of cell surface area experiencing supercritical transmembrane voltages. Curves calculated for critical minimal field strengths of 2 (○) and 3 (●) kV/cm.

the leak permeability (as probed by the leak currents) induced by electrical breakdown increases much more steeply with field strength [5].

An alternative explanation for the nonlinear, increase of the leak permeability with voltage might be the nonlinear increase of the fraction of the surface area of a single erythrocyte which experiences the critical transmembrane potential V_c and consequently develops leaks when the cell suspension is subjected to external fields (E_{ext}) of increasing strength. This fraction will be proportional to the leak permeability, as a fraction of the maximal leak permeability, if it is assumed that leak permeability is produced by structural defects occurring at constant density per unit of surface area. This fraction may be calculated as outlined in the Appendix. Its logarithm can be plotted as a function of the field strength applied in excess over the minimal critical field strength E_{min} just leading to cell damage.

The resulting relationship is shown in Fig. 9. Although the curve is somewhat biphasic it does not exhibit any quantitative relationship to our experimental data in Fig. 3. It predicts that 50% of the maximally obtainable permeability is already induced by voltages exceeding the critical minimal field strength (2–3 kV/cm at $\tau = 40$ μs [7,9]) by not more than 2–3 kV/cm. From our experimental data (Fig. 3), it becomes evident that the in-

duced leak can at least be increased by a factor of 10 when the field strength is increased from, say, 6 kV/cm to the maximal value of 10 kV/cm studied at a pulse length of 40 μs. Factors related to cell geometry alone can thus not account for the exponential increase of leak permeability.

This conclusion does not only apply to models in which a field vector perpendicular to the plane of the membrane causes the structural alteration, but also to concepts involving a vector operative parallel to the plane of the membrane, e.g., by inducing a lateral displacement of membrane proteins (see below) leading to leak formation.

(c) The slopes of the log leak permeability/voltage relationship and in particular their position in the coordinate system vary with the duration of the electric pulse. By replotting the experimental data, it can be demonstrated that a hyperbolic relationship exists between E_D and τ (Fig. 10). To obtain a certain leak permeability a constant value of the product $\tau \cdot E_D$ is thus required. A similar relationship was already shown for the critical minimal field strength [7,9]. It is obviously also valid in the supercritical range.

Influence of ionic strength during breakdown

The ionic strength of the suspension medium

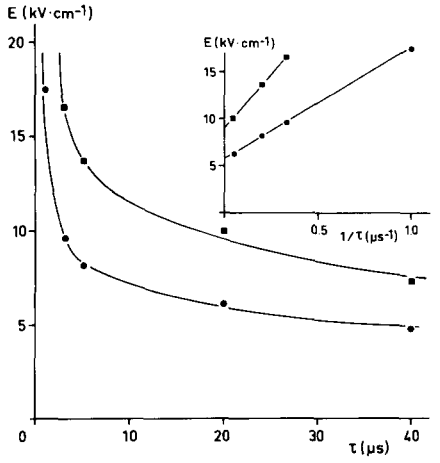

Fig. 10. Hyperbolic relationship between field strengths and pulse lengths required to obtain a leak permeability $P' = (t_{H_{50}})^{-1}$ of a constant given magnitude. (●) $P' = 0.05$ min^{-1} (below the break); (■) $P' = 0.5$ min^{-1} (above the break). The inset defines the minimal breakdown voltage required to obtain a certain leak permeability.

during breakdown affects the extent of leak formation (Table I). Surprisingly, an increase of ionic strength enhances the leak. This excludes simple interpretations in which a high ionic strength would shield charged membrane components from the electric field. On the contrary, charge-screening seems to facilitate leak formation, possibly as a consequence of a reduction of repulsive forces between membrane elements (proteins, phospholipid headgroups). Such repulsive forces might counteract an aggregation of membrane material leading to leak formation. Alternatively, changes of the dielectric or the geometric properties of the lipid bilayer might play a role [25].

Pore size and number

Conceptually, an increase of the leak permeability with increasing breakdown voltage will result either from an increase in the number or in the size of the structural defects acting as pores, or from both effects. It has previously been claimed, that it is in particular the pore size that increases with increasing voltages [7]. We reinvestigated this issue by analysis of equivalent (apparent) pore radii, using two approaches.

Relative permeabilities of small, homologous polyhydroxy compounds were evaluated in terms of the Renkin-Pappenheimer concept of restricted diffusion [26]. The data could be fitted to an equivalent pore radius between 0.55 and 0.65 nm (Fig. 11A). These numbers pertain to breakdown voltages of 6 and 8 kV/cm and do not indicate any major differences in the radii, although membrane permeabilities differ by a factor 2 at the two voltages. If this increase of permeability would arise from a mere increase of pore size we could expect an increase of the apparent radius by a factor of 1.4, which should not escape detection.

Pore sizes for a greater range of breakdown voltages were obtained by studying the protective action of compounds varying in size between $r_{SE} = 0.6$ and 1.9 nm. The results (Fig. 6) indicate that in the range of low voltages the increase in field strengths goes along with a moderate increase in pore radius, while at higher field strength this increase is more pronounced. It is therefore tempting to speculate that below the break in the leak permeability/voltage relationship the increase of leak permeabilities is due to an augmented

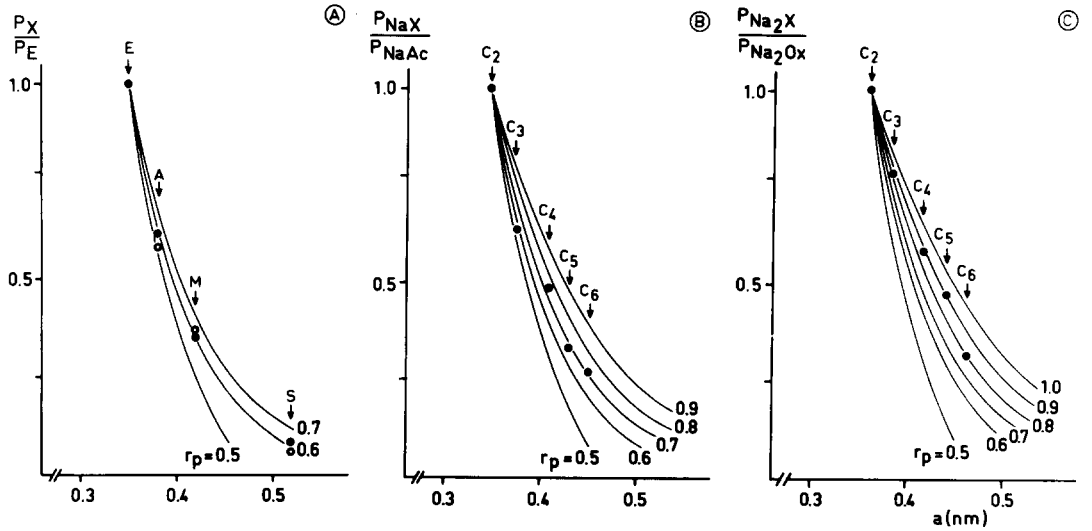

Fig. 11. Equivalent pore radii (r_p) of erythrocytes subjected to electrical breakdown, as derived from permeabilities given in Tables II and III. Values normalized to those for erythritol (A), acetate (B) or oxalate (C). The continuous lines are theoretical slopes for the expected relationship between relative permeabilities of compounds with increasing permeability through cylindrical pores with radii (nm) given at each curve. a, radius of test solute (Data from Refs. 17 and 40).

number of pores, while above the break the increase of leak permeability is the result of an additional pore enlargement.

In general, our data indicate that dielectric breakdown produces defects in the erythrocyte membrane increasing in radius from 0.6 to 1.9 nm between 4 and 10 kV/cm. The pore dimensions are thus equivalent to the areas occupied by 1–4 phospholipid molecules. The radii are of the same order of magnitude as those proposed by Kinosita and Tsong [9] but lower than radii discussed by Benz and Zimmermann [2]. They are certainly much smaller, in the range of voltages and pulse lengths studied here, than the leaks in erythrocytes undergoing osmotic lysis [27].

For any concept concerning the nature of the defects, information on the approximate number of pores would be interesting. Such numbers may be derived from permeabilities and pore radii, if assumptions are made on the diffusion coefficient within the pore, D_p, and the length of the pore, l_p. Assuming l_p to be 5 nm and D_p to be equal to diffusion coefficients in bulk water, one can calculate the total pore area per cell and from this the apparent number of pores per cell. Values derived from leak permeabilities for erythritol and K^+ are compiled in Table V. The total pore areas that can account even for considerable leak permeabilities (leading to lysis within less than 1 min) are remarkably small. They constitute at best a fraction of $2 \cdot 10^{-8}$ of the total cell surface area. The same is true for the numbers of pores. In case of K^+, 1–4 pores per cell can account for the leak flux; in case of erythritol, even a number below 1. Between 4 and 7 kV/cm, the number of pores increases by a factor of 4–5. At higher voltages, the choice of greater pore radii leads to a diminution of pore numbers. All these small numbers seem unreasonably low in view of the underlying membrane modification, which is likely to extend over the whole cell surface area, at least at high voltages. Therefore, one might speculate that the diffusion coefficients inside the pore are much lower (or the general diffusion resistance of the pore much higher) than we assume. More likely, it would seem conceivable that the membrane leaks are not static and stable. They might rather result from migrating structural defects appearing and disappearing at varying intervals. The leaks would thus be comparable to the packing defects assumed to be responsible for the loss of barrier properties in mixed lipid/protein systems (Ref.

TABLE V

CHARACTERISTICS OF THE POSTULATED PORE EQUIVALENTS INDUCED IN THE ERYTHROCYTE MEMBRANE BY ELECTRICAl BREAKDOWN

Leak permeabilities calculated for erythritol from tracer fluxes in Fig. 4 and for K^+ from data in Fig. 2 using equivalent pore radii derived from Figs. 6 and 11.

	Field strength ($kV \cdot cm^{-1}$)	Leak permeability ($10^{-7} cm \cdot s^{-1}$)	Total pore area ($10^{-14} cm^2$)	Equivalent pore radius (nm)	Apparent number of pores/cell
Tracer fluxes (erythritol)	4	0.111	0.20	0.55	0.2
	6	0.431	0.78	0.60	0.7
	7	0.724	1.31	0.65	1.0
	8	1.044	1.89	1.00	0.6
	9	1.723	3.13	1.50	0.4
K^+ net flux	4	0.79	0.96	0.55	1.0
	6	2.67	3.27	0.60	2.9
	7	4.72	5.71	0.65	4.3

39). A high probability for the occurrence of such fluctuating defects would be the primary consequence of the electrical damage to the cell membrane.

Ion selectivity

In order to characterize the ion selectivity of the induced leaks, rates of colloid-osmotic lysis were evaluated on a comparative scale. The merits and limitations of this approach have recently been discussed [17]. The results presented indicate that the leaks are in essence indiscriminately permeable to alkali cations. A minor increase of the alkali chloride permeation in the order LiCl < NaCl < KCl < RbCl < CsCl closely corresponds to the ratios between the bulk diffusion coefficient [17] of the salts. In contrast, sodium halides permeate at increasing rates in the order NaF < NaCl < NaBr < NaI, the sequence of decreasing hydrated radii. The selectivity is much greater than predicted by the aqueous diffusion coefficients. In this respect, too, the pores induced by electric discharges correspond to those induced by chemical modifications [17,18].

Discrimination, by the induced leaks, of the organic anions is much more pronounced than discrimination in bulk diffusion systems (cf. Table III). Various types of evaluation of the relative permeability or diffusion coefficients, i.e., their changes as a function of molecular weight, molar volume or their square or cubic roots, yield comparable monotonous relationships which do not allow to decide which of these parameters might be determinant. Interestingly, an evaluation of the relative permeabilities of the mono- and dicarboxylates in terms of the Renkin-Pappenheimer model leads to equivalent pore radii (Fig. 11B, C) which are in a satisfactory agreement with the numbers obtained from the permeabilities for other solutes by other techniques (Fig. 11A).

The permeability coefficients decrease more rapidly with increasing size of anions than the diffusion coefficients. This indicates that interactions with the pore play a role in anion discrimination. This concept is further supported by the marked differences between anions of equal size but different charge (acetate/oxalate), and by the difference between differently substituted carboxylic acids of comparable size. The pK' values of such anions, i.e., their relative polarities, do not influence the transfer rates. Similar permeabilities were established for butyrate ($pK = 4.8$) and α-chlorobutyrate ($pK = 3.8$) or succinate ($pK_1 = 4.2$) and malate (α-hydroxysuccinate, $pK_1 = 3.4$). The high permeability for oxo-substituted carboxylates and for their unsaturated analogous might therefore result from hydrogen bonding or other types of interaction with the membrane. In the case of the oxo-anions, it should also be considered that ring closure between the carboxyl and the oxo

group might favorably influence the geometry of the anions. Indeed, cyclic monocarboxylates (e.g., benzoate) are more permeable than would be expected from their size as compared to aliphatic carboxylates.

The molecular nature of the structural defects acting as leaks

Summing up, the aqueous leaks induced by electric field have a voltage-dependent number and size, they discriminate ions only weakly and they are stable at low temperature. Leak formation is also paralleled by a pronounced increase of the transbilayer mobility of phospholipids and a partial loss of phospholipid asymmetry [28]. Furthermore, electrical breakdown of a membrane induces fusion of cells brought into close contact [1,11]. Such fusion requires considerable reorganization in the lipid domain. Therefore, it seems very likely that membrane lipids are involved in leak formation. On the other hand, the remarkable stability of the leaky state, at least at low temperature, argues against a purely lipidic origin of the leak. It would seem an attractive hypothesis that protein aggregation brought about by the field pulse induces fluctuating structural instabilities in the lipid domain which serve as pores and flip sites. Similar fluctuating structural instabilities are discussed as the basis for leaks formed in the erythrocyte membrane by chemical modification [16–18,29] and an experimental insertion of lytic toxins [30]. Since the chemically induced leaks have a number of properties (e.g., ion selectivity, reversibility) in common with those induced by electrical breakdown, it seems a reasonable working hypothesis that similar structural defects are formed under all these conditions. They might be comparable to the 'leaky patches' supposed to be formed in membranes around the complement complex after its insertion into a target membrane [31].

The protein aggregates responsible for the formation of such 'leaky patches' in cells subjected to electric fields might be formed by lateral electrophoretic displacement of integral proteins during the field pulse. The principal possibility of such a phenomenon has been demonstrated for cells in culture and for mitochondria [32–34]. It will have to be established that the much shorter but also much stronger electric field pulses applied during electric breakdown experiments are sufficient to induce displacement of proteins even in the membrane of erythrocytes, in which lateral mobility of proteins is impeded [35,36] by a submembraneous skeletal protein network.

Appendix

Calculation of the fractional surface area undergoing breakdown upon application of increasing external field strengths to spherical cells

The transmembrane potential (V) induced in a spherical cell by field pulses is related to the external field strength (E_{ext}) by the Laplace equation:

$$V = E_{ext} \cdot r \cdot f \cdot \cos \vartheta \tag{3}$$

where r is the radius of the cell, f a shape factor (1.5 for a sphere) and ϑ the angle between the direction of the radius at a certain point on the cell surface and the direction of the electric field (Fig. 12).

Upon increasing E_{ext}, the critical transmembrane potential V_c will first be reached at the two poles of the cell for which $\vartheta = 0$, i.e., $\cos \vartheta = 1$. At this minimal field strength E_{min}, a minimal structure defect will occur and induce a minimal leak permeability. Upon increasing the external field strength to a value E_{act}, structural defects will occur not only at the two opposite poles of the cell ($\vartheta = 0$), but also on the surface of a segment of a spherical cell for which:

$$V_c \leqq E_{act} \cdot r \cdot f \cdot \cos \vartheta \tag{4}$$

where ϑ defines the size of the segment. From a simple geometric consideration it follows that:

$$\frac{E_{act}}{E_{min}} = \frac{1}{\cos \vartheta} \tag{5}$$

The surface area A_S of the segment defined by ϑ is described, for both hemispheres, by:

$$A_S = 4 \cdot \pi \cdot r^2 \cdot (1 - \cos \vartheta) \tag{6}$$

or, from Eqns. 5 and 6:

$$A_{rel} = \frac{A_S}{4 \cdot \pi \cdot r^2} = 1 - \frac{E_{min}}{E_{act}} \tag{7}$$

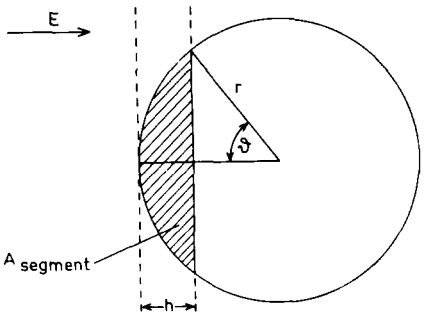

Fig. 12. Parameters determining and describing the surface segments (of a spherical cell), for which the critical membrane voltage V_c is reached at a certain value of the external field strength E.

If now we assume that the leak permeability P_{leak} induced by a supercritical external field strength E_{act} is only a function of the fraction A_{rel} of the cell surface area for which the critical transmembrane voltage V_c is reached, it follows that:

$$\frac{P_{leak}}{P_{leak\ max}} = 1 - \frac{E_{min}}{E_{act}} \tag{8}$$

where $P_{leak\ max}$ would be the leak permeability attained when the total cell surface area ($4\pi r^2$) experiences a supercritical transmembrane potential, i.e., $\vartheta = 90°$.

The relationship between leak permeability and external field strength can now be simulated, using normalized values, by plotting $1 - (E_{min}/E_{act})$, as a measure of the relative leak permeability, against $E_{act} - E_{min}$, the actual field strength applied in excess over the minimal critical field strength just leading to minimal cell damage.

Acknowledgements

This work was supported by the Deutsche Forschungsgemeinschaft (SFB 160/C3). The authors are indebted to Professor U. Zimmermann (Jülich/Würzburg) for providing some of the necessary equipment and for helpful discussions. The technical assistance of B. Müller, P. Lütkemeier and M. Sistemich is gratefully acknowledged. We thank Mrs. H. Thomas for secretarial help and Mr. F.J. Kaiser for photographic work.

References

1 Zimmermann, U. (1982) Biochim. Biophys. Acta 694, 227–277
2 Benz, R. and Zimmermann, U. (1981) Biochim. Biophys. Acta 640, 169–178
3 Teissie, J. and Tsong, T.Y. (1981) Biochemistry 20, 1548–1554
4 Zimmermann, U., Pilwat, G. and Riemann, F. (1974) Biophys. J. 14, 881–899
5 Chernomordik, L.V., Sukharev, S.I., Abidor, I.G. and Chismadzhev, Yu.A. (1983) Biochim. Biophys. Acta 736, 203–213
6 Dimitrov, D.S. (1984) J. Membrane Biol. 78, 53–60
7 Riemann, F., Zimmermann, U. and Pilwat, G. (1975) Biochim. Biophys. Acta 394, 449–462
8 Zimmermann, U., Pilwat, G., Holzapfel, C. and Rosenheck, K. (1976) J. Membrane Biol. 30, 135–152
9 Kinosita, K. and Tsong, T.J. (1977) Biochim. Biophys. Acta 471, 227–242
10 Zimmermann, U., Vienken, J. and Pilwat, G. (1980) Bioelectrochem. Bioenerg. 116, 553–574
11 Zimmermann, U., Scheurich, P., Pilwat, G. and Benz, R. (1981) Angew. Chem. 93, 332–351
12 Knight, D.E. and Baker, P.F. (1982) J. Membrane Biol. 68, 107–140
13 Kinosita, K. and Tsong, T.J. (1977) Nature 268, 438–440
14 Jausel-Hüsken, S. and Deuticke, B. (1981) J. Membrane Biol. 63, 61–70
15 Wilbrandt, W. (1941) Pfluegers Arch. Ges. Physiol. 245, 23–52
16 Deuticke, B., Lütkemeier, P. and Haest, C.W.M. (1983) Biochim. Biophys. Acta 731, 196–210
17 Deuticke, B., Lütkemeier, P. and Sistemich, M. (1984) Biochim. Biophys. Acta 775, 150–160
18 Heller, K.B., Poser, B., Haest, C.W.M. and Deuticke, B. (1984) Biochim. Biophys. Acta 777, 107–116
19 Schwister, K. and Deuticke, B. (1984) 8th International Biophysics Congress Bristol, 1984, Abstract No. 122, p. 218
20 Glynn, I.M. (1956) J. Physiol. 134, 278–310
21 Scherer, R. and Gerhard, P. (1971) J. Bacteriol. 107, 718–735
22 Perrin, D.D. (1965) Dissociation Constants of Organic Bases in Aqueous Solution, Butterworths, London
23 Gauger, B. and Bentrup, F.W. (1979) J. Membrane Biol. 48, 249–264
24 Benz, R. and Conti, F. (1981) Biochim. Biophys. Acta 645, 115–123
25 Ashcroft, R.G., Coster, H.G.L. and Smith, J.R. (1981) Biochim. Biophys. Acta 643, 191–204
26 Renkin, E.M. (1955) J. Gen. Physiol. 38, 225–243
27 Lieber, M.R. and Steck, T.L. (1982) J. Biol. Chem. 257, 11651–11659
28 Dressler, V., Schwister, K., Haest, C.W.M. and Deuticke, B. (1983) Biochim. Biophys. Acta 732, 304–307
29 Haest, C.W.M., Heller, K.B., Kunze, I.G., Schwister, K., Dressler, V. and Deuticke, B. (1983) Biomed. Biochim. Acta 42, 127–129
30 Haest, C.W.M., Schneider, E. and Deuticke, B. (1984) Hoppe-Seyler's Z. Physiol. Chem. 365, 996 (Abstr.)

31 Esser, A.F. (1981) in Biological Membranes, Vol. 4 (Chapman, D., ed.), pp. 277–325, Academic Press, London
32 Poo, M. (9181) Annu. Rev. Biophys. Bioeng. 10, 245–276
33 Sowers, A.E. and Hackenbrock, C.R. (1981) Proc. Natl. Acad. Sci. USA 78, 4246–4250
34 Zimmermann, U. and Vienken, J. (1984) in Cell Fusion (Beers, R.F. and Bassett, E.G., eds.), pp. 171–187, Raven Press, New York
35 Koppel, D.E., Sheetz, M.P. and Schindler, M. (1981) Proc. Natl. Acad. Sci. USA 78, 3576–3580
36 Sheetz, M.P., Febbroriello, P. and Koppel, D.E. (1982) Nature 296, 91–93
37 Giebel, O. and Passow, H. (1960) Pflügers Arch. 271, 378–388
38 D'Ans-Lax (1967) Taschenbuch für Chemiker und Physiker, Bd.I, Springer-Verlag, Berlin
39 Van Hoogevest, P., Du Maine, A.P.M. and De Kruijff, B. (1983) FEBS Lett. 157, 41–45
40 Schwister, K. (1985) Ph.D. Thesis, RWTH, Aachen